ELSEVIER

Global and Planetary Change 13 (1996) 117–134

GLOBAL AND PLANETARY CHANGE

Description of the Biosphere–Atmosphere Transfer Scheme (BATS) for the Soil Moisture Workshop and evaluation of its performance

Zong-Liang Yang *, Robert E. Dickinson

Institute of Atmospheric Physics, University of Arizona, Tucson, AZ 85721 USA

Received 5 May 1995; accepted 28 August 1995

Abstract

This paper has two major emphases. First, a concise description of the framework of the Biosphere–Atmosphere Transfer Scheme (BATS) is given to help better understand the results of research including BATS. Focus is put on the formulations of drag coefficients, soil surface evaporation, infiltration, surface runoff, drainage, soil internal water fluxes, canopy interception loss and transpiration, and soil water budgets. Secondly, the simulations from BATS using the default parameters are compared with those using the parameters provided during the workshop, as well as with observations. The simulations of soil moisture content from these two sets of parameters are similar, and are both in agreement with observations. In particular, the model results are discussed in the context of the applicability of the demand–supply approach. We have examined the model's sensitivity to the parameters in the formulations of runoff components. The excessive surface runoff can be fixed using a modified scheme for surface runoff. When the averaged soil moisture threshold is close to field capacity, the modified surface runoff scheme produces results essentially identical to the default scheme. With the modified scheme, in which the averaged soil moisture threshold is set to unity, the best simulation of annual evaporation and runoff components has to be obtained at the expense of the soil moisture content in the bottom layer.

1. Introduction

The development of the Biosphere–Atmosphere Transfer Scheme (BATS) is well documented in Dickinson et al. (1981), Dickinson (1984), Dickinson et al. (1986) and Dickinson et al. (1993). Originally, BATS was designed for use in the National Center for Atmospheric Research (NCAR) Community Climate Model (CCM). But its philosophy, as well as many aspects of its physical parameterizations, have been adopted in other land-surface models (LSMs) developed for use in various general circulation models (GCMs) (e.g., Sellers et al., 1986, 1995; Noilhan and Planton, 1989; Pitman et al., 1991; Liang et al., 1994). Dickinson and Kennedy (1991) have evaluated the performance of land surface hydrology from BATS as coupled to the NCAR CCM,

* Institute of Atmospheric Physics, PAS Building #81, The University of Arizona, Tucson AZ 85721, USA. Phone: + 1 520 621 6619; Fax: + 1 520 621 6833; E-mail: zly@frost.atmo.arizona.edu.

SSDI 0921-8181(95)00041-0

Version 1. Dickinson and Henderson-Sellers (1988) have used one early version of BATS coupled to CCM to investigate the regional climatic impacts of tropical deforestation. In addition, BATS is also used in high-resolution regional climate models (e.g., Giorgi et al., 1993).

Adopting some of the approaches of Deardorff (1978) in the soil temperature formulations and in the treatment of the vegetation interception, Dickinson et al. (1981) developed a well-balanced, soil–vegetation–snow–atmosphere transfer scheme suitable for GCMs. In the 1981 version, there are 10 prescribed land cover types. For each grid-square, the vegetation type is determined by a number of parameters including albedo, surface roughness length, vegetation cover, leaf area index, stem area index and stomatal resistance. Dickinson (1984) further improved the representation of evapotranspiration and made it more general for use in large-scale climate models by including a physically based soil hydrology scheme and conceptually realistic formulations of various aerodynamic and surface resistances. In Dickinson et al. (1986), there was a significant improvement in the assignment of land cover types, soil types and their parameters based on one of the best available global land-cover datasets (Wilson and Henderson-Sellers, 1985). This refined scheme was termed the Biosphere–Atmosphere Transfer Scheme (BATS), with versions to run in both off-line and on-line modes (i.e. coupled to GCMs), as the BATS land surface scheme entered a mature stage of operational use. Dickinson (1988) generalized the force-restore treatment for heterogeneous soil layers (e.g., when snow and soil co-exist). This feature and others (e.g., an improved treatment of soil hydrology and aerodynamic resistances) are described in Dickinson et al. (1993).

In this paper, the BATS scheme is evaluated using observations made at Caumont site during the HAPEX–MOBILHY experiment. Since the amount of snow is insufficient to have a significant impact on soil hydrology and surface roughness for this site, the description of the snow sub-model is omitted here (See Yang et al., 1996, for validation of the snow sub-model in the BATS scheme). Since the aim of the workshop was centered on the bare soil evaporation, runoff, drainage, canopy transpiration, and soil moisture contents, this paper will describe the parameterizations related to these aspects in order to help the reader better understand the results concerning BATS, as presented in this issue. More detailed descriptions of the model are given elsewhere.

2. Structure of BATS

In the BATS scheme (excluding the snow sub-model), there are 3 soil layers and 1 vegetation layer, accounting for 7 prognostic variables: canopy temperature (T_c), surface soil temperature (T_{g1}), subsurface soil temperature (T_{g2}), surface soil water (S_{sw}), root-zone soil water (R_{sw}), total soil water (T_{sw}), and canopy water store (W_{dew}). There are 18 surface-cover types which are based on Olson et al. (1983), Matthews (1983) and Wilson and Henderson-Sellers (1985). The soil type data are based on Wilson and Henderson-Sellers (1985). For each vegetation type, there are about 27 derived parameters which determine the morphological, physical and physiological properties of vegetation and soil (see Table 1).

2.1. Drag coefficients

The drag coefficients in BATS are derived from a conceptual aerodynamic resistance model, based on micrometeorological theory (e.g., Gates, 1980; Brutsaert, 1982). They are expected to work reasonably well for a single site, and may be also adequate for a GCM scale. Observational estimates of these drag coefficients at different scales are needed to test the validity of the conceptual framework as detailed below.

For a grid-square assuming a partial vegetation coverage, the effective height of reference level for calculating drag coefficients is

$$z = (z_r - d) A_v + z_r (1 - A_v) \tag{1}$$

Table 1
List of default parameters in BAS to crop/mixed farming and loamy type of soil

Parameter	Value
W_w	0.30
P_{or}	0.45
ϕ_0 (m)	0.2
K_0 (m s^{-1})	8.9×10^{-6}
B	5.5
Z_u (m)	0.1
Z_r (m)	0.5
Z_t (m)	1.6
R_{t1}	0.3
k_T	1.1
r_{smin} (m s^{-1})	120
z_{0c} (m)	0.06
d (m)	0.00
D_c (mm)	0.1
A_{v0}	0.85
S_v	0.6
LAI_{max}	6
LAI_{min}	0.5
SAI	0.5
f_{vis} (m^2 W^{-1})	0.02
D_f (m$^{-1/2}$)	10.0
$\alpha_{c,vis}$	0.1
$\alpha_{c,nir}$	0.3
I_{clr}	2

W_w = permanent wilting point, P_{or} = soil porosity, ϕ_0 = minimum soil suction, K_0 = maximum hydraulic conductivity, B = Clapp and Hornberger "B" parameter, Z_u = depth of top soil layer, Z_r = rooting depth, Z_t = total soil depth, R_{t1} = fraction of total roots in top soil layer, k_T = ratio of soil thermal conductivity to that of loam, r_{smin} = minimum stomatal resistance, z_{0c} = canopy roughness length, d = canopy zero displacement height, D_c = interception capacity per unit projected area, A_{v0} = maximum value of vegetation cover fraction, S_v = seasonal range of vegetation cover fraction, LAI_{max} = maximum leaf area index, LAI_{min} = minimum leaf area index, SAI = stem area index, f_{vis} = light sensitivity factor used in calculating the dependence of stomatal resistance on visible solar flux, D_f = inverse square root of leaf dimension, $\alpha_{c,vis}$ = canopy visible aldebo, $\alpha_{c,nir}$ = canopy infrared albedo, I_{clr} = soil color index.

where z = effective height of reference level, z_r = height of the lowest model level of the host GCM, d = zero displacement height, and A_v = fraction of vegetation coverage.

The surface bulk Richardson number is

$$R_{iB} = R_{iB,n}/V_r^2 \tag{2}$$

where

$$R_{iB,n} = gz\left[T_r - A_v T_a - (1 - A_v)T_{g1}\right]/T_r \tag{3}$$

and

$$V_r = \sqrt{u_r^2 + v_r^2 + u_{min}^2} \tag{4}$$

In these equations, u_r, v_r and T_r are wind components and temperature at z_r. T_a is temperature of canopy air space, T_{g1} is the surface soil temperature, and

$$u_{min} = \begin{cases} 1.0 \quad \mathrm{ms}^{-1} & R_{iB,n} \le 0 \\ 0.1 \quad \mathrm{ms}^{-1} & R_{iB,n} > 0 \end{cases}$$

The drag coefficient is a function of C_{Dn}, the drag coefficient for neutral stability, and R_{iB}, i.e.,

$$C_D = \begin{cases} C_{Dn}\left[1 - 12.5R_{iB}/(1 + 75C_{Dn} \quad \sqrt{-R_{iB}(z_r - d)/z_{0c}}\,\right] & R_{iB} \le 0 \\ C_{Dn}/\left[1 + 10R_{iB}(1 + 8R_{iB})\right] & R_{iB} \ge 0 \end{cases} \tag{5}$$

These forms are consistent with those used in NCAR CCM2 (Hack et al., 1993). There is a constraint on the drag coefficient, $C_D \ge \max(0.25C_{Dn}, 6 \times 10^{-4})$. The neutral drag coefficient is calculated as

$$C_{Dn} = A_v\{k/\ln[(z_r - d)/z_{0c}]\}^2 + (1 - A_v)[k/\ln(z_r/z_{0b})]^2 \tag{6}$$

where k is the von Karman taken to be 0.378, z_{0c} = roughness for canopy, and $z_{0b} = 0.01$ m, as the roughness for bare soil.

2.2. Soil surface evaporation

It is difficult to develop a formulation of soil surface evaporation that is adequate for all soil textures, soil moisture conditions, and weather regimes. Shuttleworth (1993) has reviewed the physical basis of evaporation, and its estimation and measurement. In the BATS scheme, the soil surface evaporation is calculated by using a demand–supply approach (Dickinson, 1984). Actual evaporation is the lesser of the potential evaporation (i.e., the atmospheric demand) and the maximum rate at which water can diffuse upward to a dry surface. The mathematical expression is

$$E_a = \min(E_p, E_0) \tag{7}$$

where E_a = actual evaporation, E_p = potential evaporation, and E_0 = diffusion-limited maximum evaporation.
The potential evaporation at the soil surface is

$$E_p = \rho[q_s(T_{g1}) - q_a]/r_d + \rho[q_s(T_{g1}) - q_r]/r_g \tag{8}$$

where ρ = air density, $q_s(T_{g1})$ = saturation water-vapor specific humidity at soil surface temperature T_{g1}, q_a = specific humidity of air within canopy air space, q_r = specific humidity of air at the reference level, r_d is aerodynamic resistance between ground and canopy air space, and r_g is aerodynamic resistance between ground and the reference level. Thus, the left hand side of Eq. (8) denotes evaporation from ground below canopy, and the right hand side of Eq. (8) represents evaporation from the bare portion of the ground. The areal fractions of the vegetation and the bare soil are A_v and $(1 - A_v)$, respectively. The two resistance terms are defined as

$$r_d = 1/(A_v C_{soil} V_a) \tag{9}$$

and

$$r_g = 1/[(1 - A_v)C_D V_g] \tag{10}$$

with

$$V_g = (1 - A_v)V_a + A_v[X_b V_a + (1 - X_b)V_r] \tag{11}$$

$$V_a = \sqrt{C_D}\,V_r \tag{12}$$

$$X_b = \min(1, z_{0c}) \tag{13}$$

and

$$C_{soil} = 4 \times 10^{-3}$$

The detailed form of the diffusion-limited maximum evaporation is constructed based on the behavior of a soil column, initially at field capacity, dried by a diurnally varying potential evaporation applied at the surface.

Based on the results of the multilayer soil model integrations, and on dimensional analysis and physical reasoning (Dickinson, 1984; Dickinson et al., 1993), the actual expressions are written

$$E_0 = E_{max}\overline{W}W_u \tag{14}$$

where

$$E_{max} = 1.02 D_{max} C_k / \sqrt{Z_u Z_r} \tag{15}$$

and

$$\overline{W} = W_r^{3+B_f} W_u^{B-B_f-1} \tag{16}$$

using

$$C_k = 9.76(1 + 1550 D_{min}/D_{max})[B(B-6) + 10.3]/(B^2 + 40B) \tag{17}$$

$$D_{max} = B\phi_0 K_0 / P_{or} \tag{18}$$

and

$$B_f = 5.8 - B[0.8 + 0.12(B-4)\log_{10}(100K_0)] \tag{19}$$

In these equations, Z_u = depth of the surface soil layer (restricted to be between 10 and 200 mm thickness), Z_r = depth of the soil active layer (or root zone, between 500 and 2000 mm), W_u = ratio of the surface soil layer water content to its maximum amount, W_r = ratio of the root zone soil water content to its maximum amount, P_{or} = porosity, B = a nondimensional parameter (Clapp and Hornberger, 1978), ϕ_0 = saturation soil water potential, K_0 = saturation hydraulic conductivity in mm s^{-1}, and $D_{min} = 10^{-3}$ mm^2 s^{-1}.

2.3. Wet canopy evaporation and dry canopy transpiration

In BATS, vegetation is assumed to be a flat, porous and uniform layer. The foliage is assumed to have zero heat capacity, and photosynthetic and respiratory energy transformations are neglected. The evapotranspiration from canopy consists of two separate parts: the evaporation from the water on wet foliage (leaves and stems) and transpiration from dry leaf surface. Both assume the same transfer process from the foliage surfaces to the air within canopy, except that transpiration also considers the water flux through stomata. The biophysical basis of the evapotranspiration from a canopy is reviewed in Shuttleworth (1993) and Sellers et al. (1995).

The wet canopy evaporation or interception loss is parameterized as

$$E_{dew} = \rho f_{cw}[q_s(T_c) - q_a]/r_b \tag{20}$$

where $q_s(T_c)$ = saturation water-vapor specific humidity at T_c, temperature of the canopy, f_{cw} = fractional area of canopy surface covered by water, r_b = aerodynamic resistance between canopy surface and canopy air space, and is given by

$$r_b = (A_v\, LSAI)^{-1} r_{al} \tag{21}$$

where $LSAI = LAI + SAI$, LAI = leaf area index, SAI = stem area index, and r_{al} = aero-dynamic resistance for a leaf.

The dry canopy evaporation is determined using a demand–supply approach (originally suggested by Federer, 1979), i.e.

$$E_{tr} = \min(E_{tr,dem}, E_{tr,sup}) \tag{22}$$

The transpiration by atmospheric demand is given by

$$E_{tr,dem} = \rho(1 - f_{cw})(LAI/LSAI)[q_s(T_c) - q_a]/(r_b + r_c) \tag{23}$$

where r_c = canopy surface resistance, which is a function of various environmental parameters, including species-dependent minimum stomatal resistance, solar radiation, canopy temperature and vapor pressure deficit.

The maximum supply of water by roots is determined from

$$E_{tr,sup} = A_v f_S E_{tr,max} \sum_i R_{ti}\left(1 - W_{LT}^i\right) \tag{24}$$

where $E_{tr,max}$ is an adjustable constant *with* default value, derived by Federer (1979) from New Hampshire forest data, is 2×10^{-4} mm s^{-1}; f_S, a seasonal factor, is prescribed as a quadraic function of deep soil temperature with its optimum value at 298 K (= 1 during the growing season; = 0 when the soil is frozen); and R_{ti} = the fraction of roots in a given soil layer. W_{LT}^i is defined as

$$W_{LT}^i = (\phi - \phi_0)/(\phi_{max} - \phi_0) \tag{25a}$$

$$= \left(W_i^{-B} - 1\right)/\left(W_w^{-B} - 1\right) \tag{25b}$$

where W_i = ratio of the soil water within the i-th layer to its maximum amount, W_w = the value of W at which transpiration goes to zero, ϕ = soil water potential, and ϕ_{max} = value of negative of potential of leaves at onset of desiccation. In deriving Eq. (25b), the relationship between the soil water potential and soil water content is based on Clapp and Hornberger (1978). If demand exceeds supply, then r_c is adjusted (stomatal closure) so that they match.

2.4. Infiltration and surface runoff

The theory of infiltration, its measurement and estimation are reviewed by Rawls et al. (1993). Accurate modelling of the infiltration of water into the soil over the area of a GCM grid-square requires knowledge of subgrid-scale surface (e.g., soil texture, vegetation distribution, soil moisture condition and slopes) and rainfall structure (Milly and Eagleson, 1982). In the BATS scheme, the infiltration, G_{w0}, is written as a residual of the surface water balance,

$$G_{w0} = P_0 + D_0 - E_a - R_s \tag{26}$$

using

$$P_0 = P(1 - A_v) \tag{27}$$

where P = precipitation, D_0 = excess water dripping from canopy, R_s = surface runoff, and is defined as

$$R_s = \gamma G_w \tag{28}$$

where

$$G_w = \max[0, P_0 + D_0 - E_a] \tag{29}$$

and

$$\gamma = \min\left[1, \left(\frac{W_u + W_r}{2}\right)^m\right] \tag{30}$$

with

$$m = \begin{cases} 1 & T_g < 273.16 \\ 4 & \text{otherwise} \end{cases}$$

The above formulation for surface runoff was not intended for local site application but was guided by the requirement that, used in a GCM, it should, on the average, give a similar amount of surface runoff as is observed. Observed surface runoff, on the global annual mean basis, is about half the total runoff (L'vovich, 1979).

2.5. Internal soil water fluxes

Rawls et al. (1993) have provided a detailed review of the theory of soil water movement or internal soil water fluxes. The rate of soil water movement is important in surface runoff, groundwater recharge and evapotranspiration. Computation of the internal soil water fluxes within the soil column of 1–10 m thick that is coupled to the atmosphere is difficult to implement in climate models. The reasons are due to the coarseness of the grids, usually 2–5 levels, as limited by practical considerations, and the heterogeneous distribution of topography, soil and vegetation types across the GCM grid-square.

The soil surface evaporation and the internal soil water fluxes in the BATS model are parameterized based on the multilayer soil model integrations. The capillary movement of water from the rooting zone into the surface soil layer is given by

$$\Gamma_{w1} = l_1 E_{max}(Z_u/Z_r)^{0.4}\overline{W}(W_r - W_u) \tag{31}$$

and from the total column into the rooting zone is

$$\Gamma_{w2} = l_2 E_{max}(Z_u/Z_r)^{0.5} W_t^{B_f+2} W_r^{B-B_f}(W_t - W_r) \tag{32}$$

where W_t = ratio of soil water content within the total column to its maximum amount. The gravitational drainage from the surface soil layer to rooting zone is

$$G_{w1} = l_1 K_0 W_r^{B+0.5} W_u^{B+2.5} \tag{33}$$

and from the rooting zone to the total column is

$$G_{w2} = l_2 K_0 W_t^{B+0.5} W_r^{B+2.5} \tag{34}$$

where

$$l_1 = \begin{cases} 0 & T_g \le 273.16\text{K} \\ 1 & \text{otherwise} \end{cases}$$

and

$$l_2 = \begin{cases} 0 & \text{permafrost or ice sheet} \\ 1 & \text{otherwise} \end{cases}$$

2.6. Base flow and saturation excess

Mosley and McKerchar (1993) have reviewed base flow and other components of streamflow, such as surface runoff and interflow. Pilgrim and Cordery (1993) have summarized processes and modelling of flood runoff. The base flow is drainage out of the modeled soil lower boundary. In BATS, the rate of gravitational drainage of soil water from the total soil column to underlying ground water is

$$R_{base} = l_2 K_D W_t^{2B+3} \tag{35}$$

where K_D is an adjustable constant taken to be 4×10^{-4} mm s^{-1}. The possibility of a gradient-driven upward water flow from an underlying saturated zone is neglected. The soil water content within the total soil column is checked every time step to ensure that it does not exceed its maximum amount. If the excess does occur, it is added to the total runoff and the total soil water content is set to its maximum value. Thus, the rate of the excess is written as

$$R_{excess} = \max[0, (T_{sw} - P_{or} Z_t)/\Delta t] \tag{36}$$

where T_{sw} = soil water content within the total soil column, Z_t = thickness of the total soil column, and Δt = time step. The total runoff is thus defined as

$$R_{tot} = R_s + R_{base} + R_{excess} \tag{37}$$

2.7. Soil moisture rate equations

The soil water budgets are accounted for in three layers, each extending to a different depth but all with the same top surface at the soil–air interface. The governing equations for the soil moisture contents, in the absence of snow, are parameterized as

$$\frac{\partial S_{sw}}{\partial t} = P(1 - A_v) - R_s + \Gamma_{w1} - G_{w1} - \beta E_{tr} - E_a + D_0 \tag{38}$$

$$\frac{\partial R_{sw}}{\partial t} = P(1 - A_v) - R_s + \Gamma_{w2} - G_{w2} - E_{tr} - E_a + D_0 \tag{39}$$

$$\frac{\partial T_{sw}}{\partial t} = P(1 - A_v) - R_s - R_g - E_{tr} - E_a + D_0 \tag{40}$$

where S_{sw} = surface soil water representing water in the upper layer (depth Z_u) of soil, R_{sw} = water in the rooting zone Z_r of soil, T_{sw} = total water in the soil to depth Z_t, and β = fraction of transpiration from the top soil layer.

3. Performance of BATS with default and workshop parameters

The HAPEX–MOBILHY data used in this study were collected at Caumont. Detailed information concerning the site can be found elsewhere in this issue. The vegetation type is a soya crop field, and the soil is loam. The BATS scheme has a vegetation class as crop/mixed farming and a soil type class as loam, both approximately corresponding to the features of the site. Since the default BATS parameters are those currently being used in CCM2 integrations, it is interesting to examine the performance of BATS when the default parameters are applied to this site. Values of these parameters are given in Table 1.

The BATS scheme, with its default parameters, is capable of producing realistic simulations of soil moisture in three layers: surface layer, rooting zone and total column (see Fig. 1). The wet period during the winter, the drying during the growing phase (day 120–day 210), and the dry period (day 210–day 300) are well captured. Also shown in Fig. 1 are the results from simulations using vegetation and soil parameters provided during the workshop for Experiment 15 (see Shao and Henderson-Sellers, 1996-this issue). Values assigned to these parameters were not based on the field measurement, because they were not available. Rather, they were based on an intellectual guess (cf. Shao et al., 1994) from all the information available. Interestingly, the results from using the default and ''workshop'' parameters are similar, though the simulations with the default are marginally better during the dry period, especially for rooting zone soil moisture.

The immediate implication of this is that, given the unknown nature of the parameters for this site, any reasonable combinations of values of the parameters can reproduce the observed soil moisture content. This does not mean that the model is not sensitive to some parameters. In fact, the model is sensitive to vegetation cover fraction, leaf area index (*LAI*), stem area index and roughness length, to mention a few. Considering the

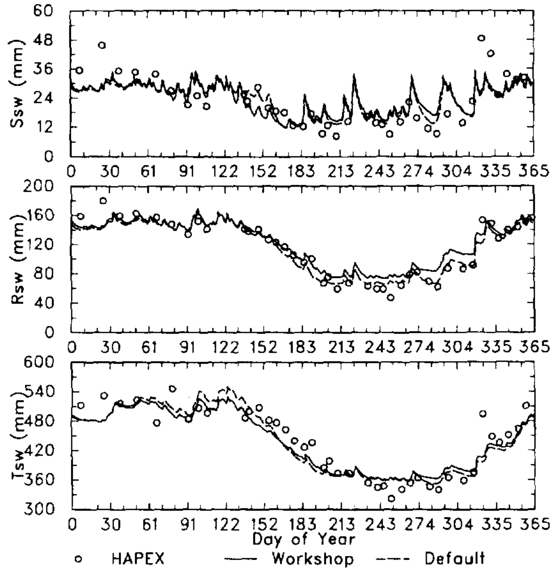

Fig. 1. Daily averages of soil water content for three-layers as simulated by the BATS model compared with HAPEX data (weekly measurements). The same layers apply to both simulated and observed. The simulated results are shown for two runs, one with default parameters, the other with parameters provided during the workshop.

residual of vegetation (e.g., weeds), before and after growing seasons (i.e. days 121–270), as the case in the default (see Fig. 2), leads to an overall reduction in latent heat flux (but increase in sensible heat flux) before the growing season for the run with the default (see Fig. 3). The existence of residual vegetation may be realistic for

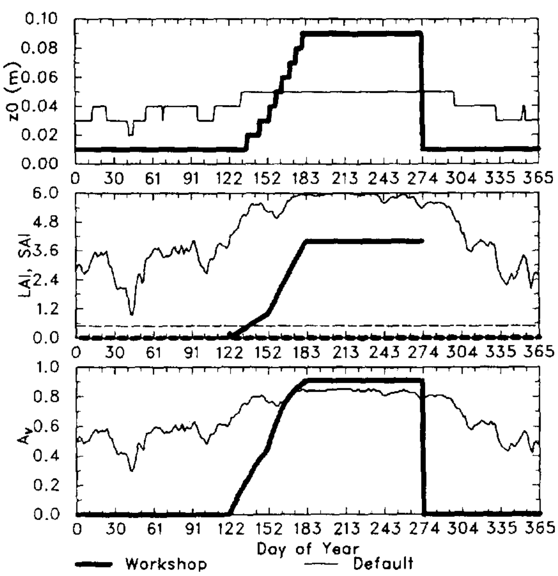

Fig. 2. Annual sequence of daily mean surface roughness (top panel), leaf area index (LAI) and stem area index (SAI) (middle panel), and vegetation cover fraction (bottom panel) for two runs, one with default parameters (thin lines), the other with parameters provided during the workshop (thick lines). The solid lines in the middle panel refer to LAI, while the dashed lines are for SAI.

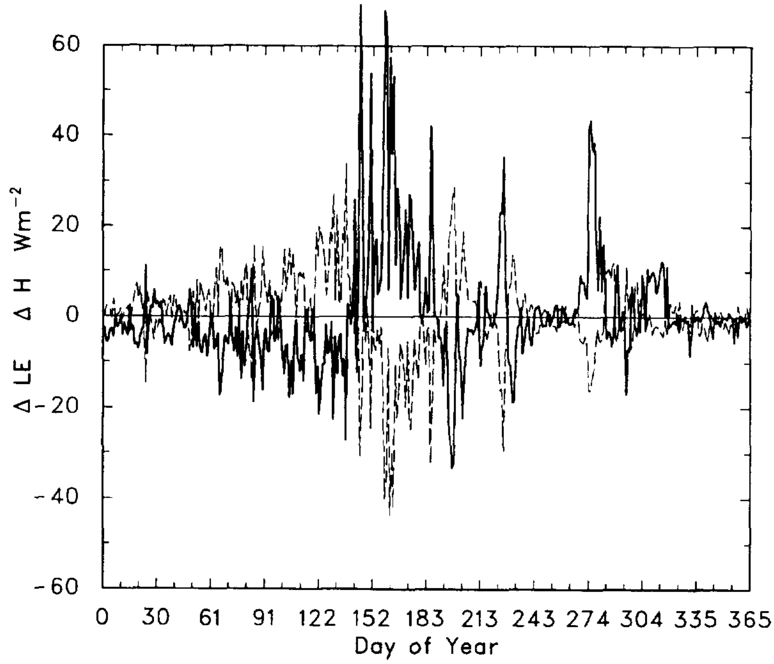

Fig. 3. Annual sequence of differences in latent heat fluxes (solid line) and sensible heat fluxes (dashed line), between the run with default parameters and the run with parameters provided during the workshop.

agriculture fields, and even more so on the GCM scale. During the early stage of the growing phase (i.e., days 140–180) (Fig. 2), the larger LAI and vegetation cover fraction in the default result in an enhanced latent heat flux (but decreased sensible heat flux) for that period (Fig. 3). An inverse modelling starting with the observed data, plus an optimization package such as those reviewed by Feddes (1995), could be used to produce a unique set of parameter values, but these values might not be physically reasonable. In view of this, it would be inappropriate to consider the parameters introduced during the workshop as a permanent change to be introduced in BATS.

The simulated fluxes versus those observed for two particular periods are shown in Figs. 4 and 5. During the first period (i.e., Days 148–157 or May 28–June 6), when the soil is relatively humid (see Fig. 1), the simulated fluxes from the default and workshop parameters are broadly similar, but the results from the default are in closer agreement with the observed (Fig. 4). Such an improvement corresponds to an increase in latent heat flux by as high as 70 W m^{-2}. Both versions fail to simulate the dew formed on the canopy surface during the night. For the second period (i.e., Days 175–184 or during June 24–July 3), when the soil is drier, with water content close to the wilting point, the simulated latent fluxes are underestimated when there is a strong solar forcing, but are in close agreement with the observed when the solar forcing is weak (Fig. 5). The main reason for these large differences is that the transpiration is calculated using demand–supply approach (see Eqs. 22–24). When the net radiation is large, the atmospheric demand of transpiration is high, whereas the rate of supply that the soil water could be transferred through roots is low. Thus, the actual calculated transpiration is determined by the rate of supply. This is clearly evident at noon during summer (see Fig. 5). In case of weak solar radiation (e.g., during cloudy days), the atmospheric demand declines, and the soil water supply through the roots could keep up with the demand, and the simulations are comparable to the observed.

The disagreement in evapotranspiration during the midday stress period suggests the need to adjust, for this case, some of the parameters used in the root supply parameterizations, by either increasing $E_{tr,max}$, or changing the distribution of roots. Returning to Fig. 1, the simulated soil moisture in the surface layer is overestimated

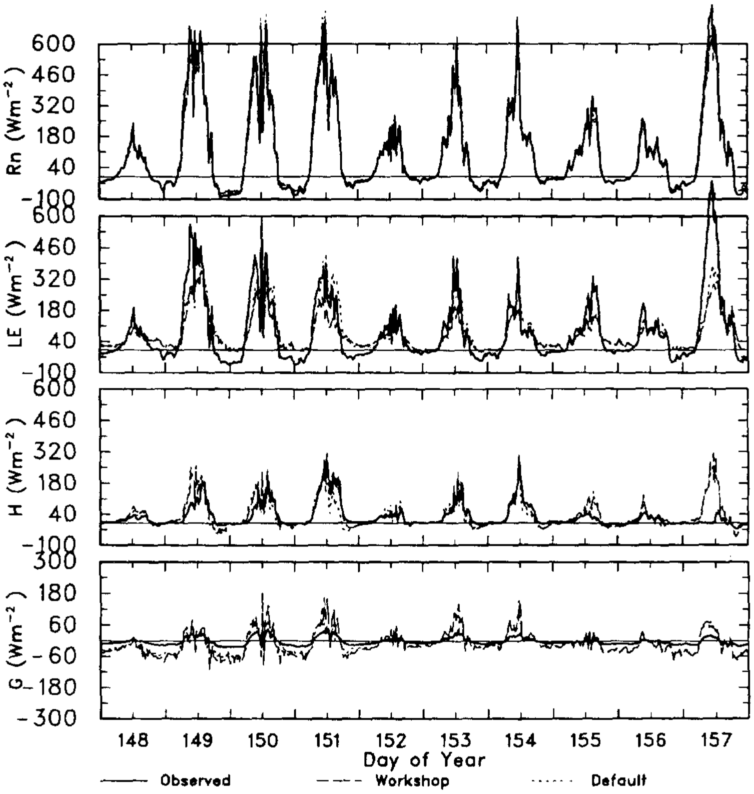

Fig. 4. Simulated diurnal variations of net radiation (top panel), latent heat flux (second panel), sensible heat flux (third panel), and ground heat flux (bottom panel) compared with the observed. The simulated results are shown for two runs, one with default parameters, the other with parameters provided during the workshop. The results are shown for a period from Days 148–157 (or May 28–June 6).

during the dry period (day 210–day 300), whereas the root-zone soil water is close to the observed, i.e. at the wilting point. Since the root fraction in the top layer is specificed as 0.3 throughout the integration with the default parameters, this may not be realistic when the whole root-zone is water limited while the surface water appears more than adequate.

4. Sensitivity to parameterizations of surface runoff and drainage

Shao et al. (1994) have compared the simulations of the accumulated surface runoff from 14 models as a function of the day of the year (see their fig. 11). BATS is the only model that gives a large surface runoff, accounting for about 19% of annual precipitation, while the other models predict the near zero surface runoff, in accord with the observational estimates. In addition, Shao et al. (1994) have shown that ten of the 14 models underestimate total runoff, but overestimate evaporation (see their fig. 31). In terms of total runoff, BATS lies in the middle of this group of ten models. It is thus of interest to examine how the runoff process in BATS works and is linked to the soil moisture profiles and evaporation. Referring to Eqs. (30) and (35), m and K_D, two adjustable constants, are used in formulations of surface runoff and base flow, respectively. We might expect both m and K_D to change with locations where elevation, slope, and vegetation and soil types are different. In the current BATS model, $m \equiv 4$ for non-frozen soil, and $K_D \equiv 4 \times 10^{-4}$ mm s^{-1}. We are seeking a

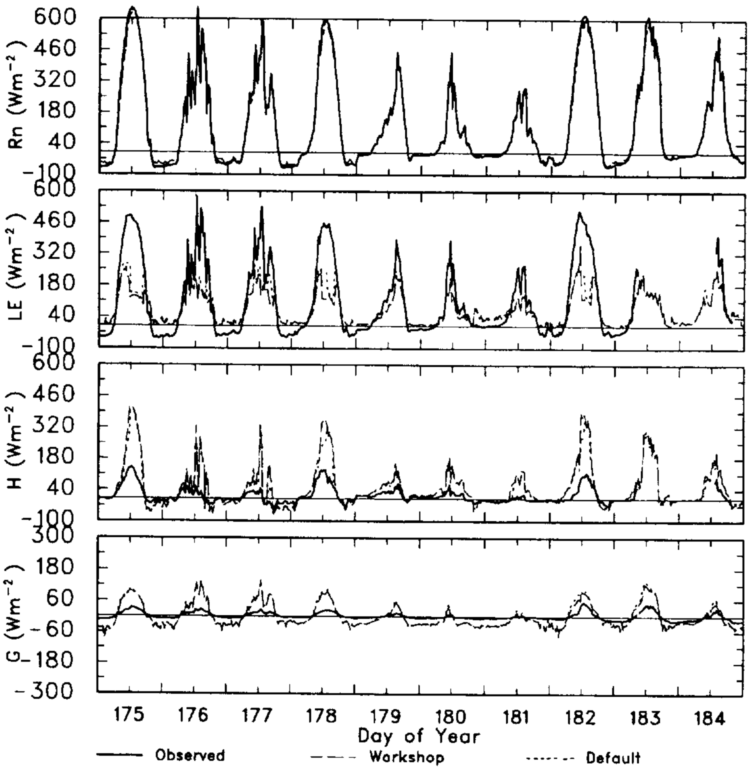

Fig. 5. As in Fig. 4, but for a period from Days 175–184 (or June 24–July 3).

relationship between the model's performance (in terms of simulations of soil moisture, runoff components and evaporation) and a wide range of possible values of m or K_D.

Fig. 6 shows the root-mean-square-error (RMSE) (this includes both time fluctuation and mean bias) of soil moisture profiles as a function of m, over the range 0–20, where 4 is the default value in the model. The lowest RMSE means the best performance. It turns out that the value of 4 is a very good choice, though the best value for T_{sw} would be 5, for R_{sw} 3 and S_{sw} 6, but the differences are negligible when m is greater than or equal to 4. Fig. 7 depicts the Spearman rank-order correlation coefficient (cf. Press et al., 1992) between modeled and observed as a function of m. It shows, except for S_{sw}, that deeper layer soil water contents are insensitive to m when $m \geq 1$. The correlation coefficient is generally higher for the deeper soil water simulations.

Fig. 8 shows the annual accumulated evaporation and runoff components as a function of m. As m increases beyond 4, total runoff and evaporation are very close to steady states, while changes in surface runoff and base flow (drainage) cancel each other. To get the zero surface runoff, in agreement with observations, m has to be rather large (i.e., ≥ 20). To match the observational estimates of annual total runoff (241 mm/yr) or annual evaporation (615 mm/yr), m has to be set to 2.75, close to the default value of 4.

Another parameter, K_D, links drainage or base flow with soil moisture content within the total soil column (Fig. 9). Over a large range of change in K_D, there is little change in RMSE of S_{sw} and R_{sw}, but with a considerable error in T_{sw} when K_D is greater than default value. For evaporation and runoff (Fig. 10), there is a small change of about 50 mm/yr in surface runoff, but there is a large increase in drainage from 0 mm to about 200 mm/yr for the whole range of K_D, correspondingly, a large increase in total runoff. To reproduce observational total runoff or evaporation, we need to increase K_D by a factor of about 10.

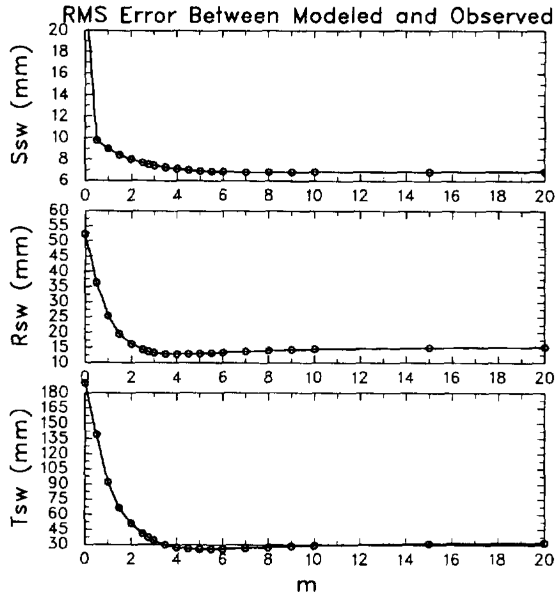

Fig. 6. The root-mean-square-error of S_{sw} (top panel), R_{sw} (middle panel) and T_{sw} (bottom panel), as a function of m.

We now propose an alternative method of treating surface runoff, by explicitly including the two surface runoff generating mechanisms, namely, infiltration excess and saturation flow. The key here is W_a, a threshold to determine the saturation flow, that can be freely "changed". The modified approach takes the form

$$R_s = \max[0, (P_e - G_{wn})] \tag{41}$$

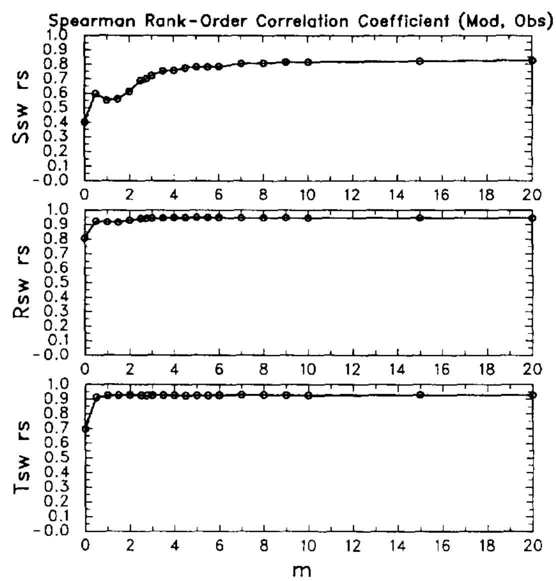

Fig. 7. The Spearman rank-order correlation coefficient between modeled and observed of S_{sw} (top panel), R_{sw} (middle panel) and T_{sw} (bottom panel), as a function of m.

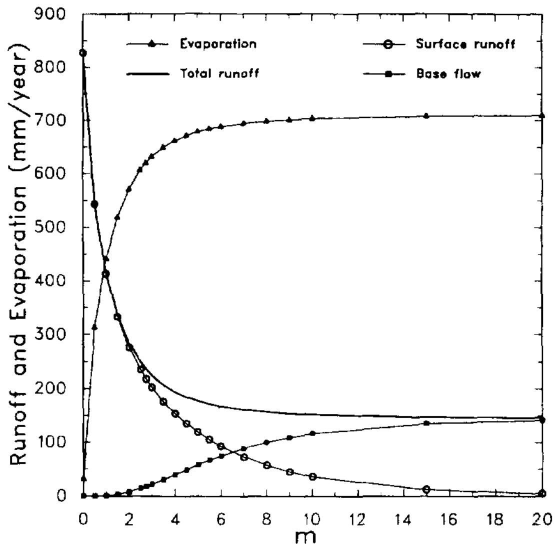

Fig. 8. The annual total evaporation and runoff components as a function of m.

where $P_e = P_0 + D_0$ = effective precipitation on soil surface; G_{wn} = infiltration of precipitation into the surface layer and the root zone, and is

$$G_{wn} = \begin{cases} \min(P_e, K_s) & 0.5(W_u + W_r) < W_a \\ 0 & 0.5(W_u + W_r) \geq W_a \end{cases} \tag{42}$$

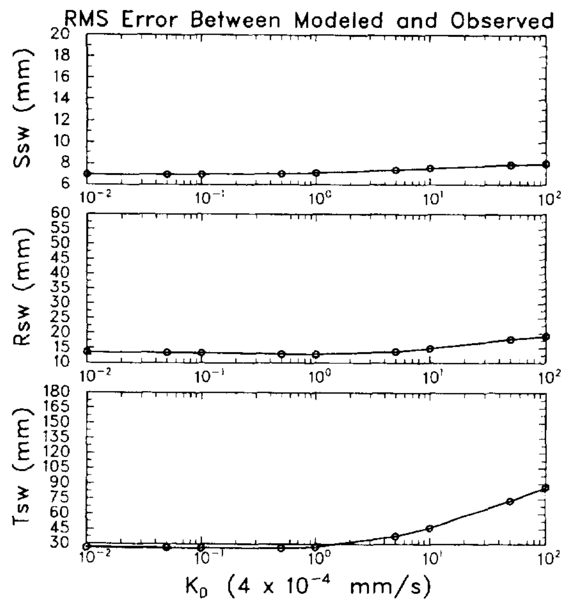

Fig. 9. The root-mean-square-error of S_{sw} (top panel), R_{sw} (middle panel) and T_{sw} (bottom panel), as a function of K_D, which ranges from a factor of 100 smaller to a factor of 100 greater than the default value, 4×10^{-4} mm s^{-1}.

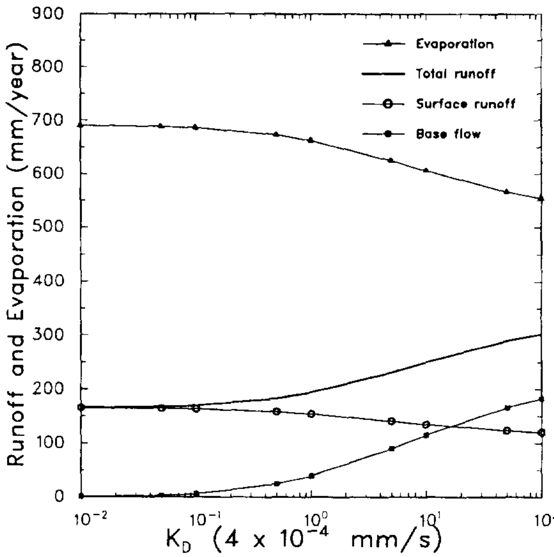

Fig. 10. The annual total evaporation and runoff components as a function of K_D, which ranges from a factor of 100 smaller to a factor of 100 greater than the default value, 4×10^{-4} mm s^{-1}.

where K_s = hydraulic conductivity of saturated soil. Equation (42) states that when the averaged soil moisture content, i.e., 0.5 $(W_u + W_r)$, is greater than a threshold, infiltration is zero, and that when the averaged soil moisture content is less than the threshold, infiltration is the lesser of effective precipitation input and saturation hydraulic conductivity. Variable W_a, the averaged soil moisture threshold, may be adjusted for a wide range of applications, from local site to the GCM scale.

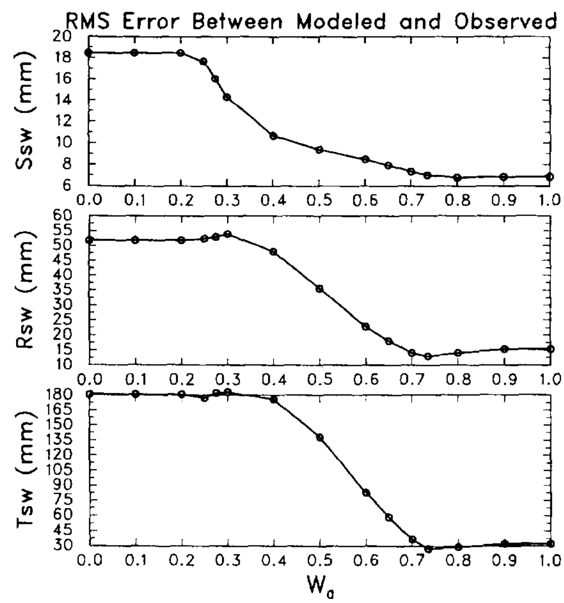

Fig. 11. The root-mean-square-error of S_{sw} (top panel), R_{sw} (middle panel) and T_{sw} (bottom panel), as a function of W_a, the averaged soil moisture threshold.

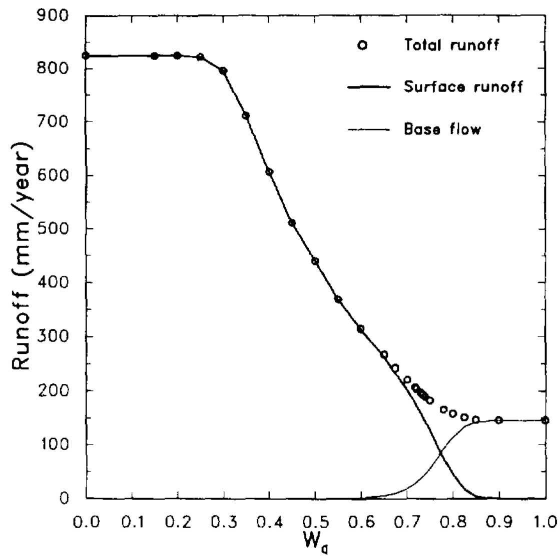

Fig. 12. The annual runoff components (total runoff, surface runoff and base flow) as a function of W_a, the averaged soil moisture threshold.

Fig. 11 shows the RMSE of soil moistures as a function of W_a. Clearly, there is a simple relationship in which the best performances correspond to 0.7 and greater. Coincidentally, the best value of 0.735 is close to the field capacity estimated for this site. Fig. 12 exhibits the components of runoff as a function of W_a. When W_a changes from 0 to 1, surface runoff ranges from 800 mm/yr (all the rainfall goes to surface runoff) to 0 mm/yr, while the base flow changes from 0 mm/yr to 150 mm/yr. The total runoff, sum of both components, ranges from 800 mm/yr to 150 mm/yr. Since water is balanced in terms of annual total, alternatively, this means that evaporation changes from 0 to about 650 mm/yr. When W_a is set to 0.735, the resultant annual total evaporation and runoff are identical to the values obtained from the default parameterization of the surface runoff. These results suggest that the default scheme implicitly incorporates two types of surface runoff: the infiltration excess and saturation flow.

5. Summary

In this study we have compared simulations from BATS using default and modified parameters against the observed. We find that both these sets of parameters produce similar results, and are in close agreement with observed. This is not surprising because of the unknown nature of the parameters for this site, any reasonable combinations of values of the parameters can lead to the same answer, i.e. reproduction of the observed soil moisture content. Thus, the parameters characterizing the site as given in the workshop are not considered as a permanent change for use in BATS.

Although the soil moisture is realistically simulated, the latent heat fluxes are underestimated when the soil is relatively dry. This does not, however, invalidate the demand–supply approach as employed in BATS. The underestimation is attributed, in part, to the default parameters used for root dynamics (i.e., root distribution and rooting depth as a function of available water), to the possible errors in quantification of the roots for the site, and to the difficulty in establishing the relative confidence in flux measurements and soil moisture observations. In summary, since a comprehensive set of field data for various crops over all the localities of the globe is not available, caution should be taken in any generalization as to all the crop areas in the domain of a GCM.

The current default values of m and K_D, in the parameterizations of runoff components, lead to realistic simulations of soil moisture profiles, but, unrealistic partitioning of runoff components. When the averaged soil moisture threshold is close to field capacity, the modified surface runoff scheme produces results essentially identical to the default scheme with $m = 4$. With the modified scheme, in which the averaged soil moisture threshold is set to unity, the best simulation of annual evaporation and runoff components has to be obtained at the expense of the soil moisture content in the bottom layer.

Acknowledgements

We thank Dr. Ann Henderson-Sellers for the initiative of the soil moisture workshop. Our gratitude also extends to all the scientists who contributed to collect and process the field data from HAPEX–MOBILHY. The comments from anonymous reviewers lead to improvement of this paper. This paper was completed under funding from NOAA Project NA16RC0119-01.

References

Brutsaert, W.H., 1982. Evaporation into the Atmosphere. Reidel, Boston, 299 pp.

Clapp, R.B. and Hornberger, G.M., 1978. Empirical equations for some soil hydraulic properties. Water Resour. Res., 14: 601–604.

Deardorff, J.W., 1978. Efficient prediction of ground surface temperature and moisture, with inclusion of a layer of vegetation. J. Geophys. Res., 83: 1889–1903.

Dickinson, R.E., 1984. Modelling evapotranspiration for tree-dimensional global climate models. In: J.E. Hansen and T. Takahashi (Editors), Climate Processes and Climate Sensitivity (Geophys. Monogr., 29, Maurice Ewing Vol. 5). AGU, Washington, DC, pp. 58–72.

Dickinson, R.E., 1988. The force-restore model for surface temperatures and its generalizations. J. Climate, 1: 1086–1097.

Dickinson, R.E. and Henderson-Sellers, A., 1988. Modelling tropical deforestation: A study of GCM land-surface parameterizations. Q. J. R. Meteorol. Soc., 114: 439–462.

Dickinson, R.E. and Kennedy, P.J., 1991. Land surface hydrology in a general circulation model—Global and regional fields needed for validation. Surv. Geophys., 12: 115–126.

Dickinson, R.E., Henderson-Sellers, A. and Kennedy, P.J., 1993. Biosphere Atmosphere Transfer Scheme (BATS) Version le as coupled to the NCAR Community Climate Model. NCAR Tech. Note, TN-387 + STR, 72 pp.

Dickinson, R.E., Henderson-Sellers, A., Kennedy, P.J. and Wilson, M.F., 1986. Biosphere Atmosphere Transfer Scheme (BATS) for the NCAR Community Climate Model. NCAR Tech. Note, TN-275 + STR, 69 pp.

Dickinson, R.E., Jager, J., Washington, W.M. and Wolski, R., 1981. Boundary subroutine for the NCAR global climate model. NCAR Tech. Note, NC-173 + IA, 75 pp.

Feddes, R.A., 1995. Remote sensing—inverse modelling approach to determine large scale effective soil hydraulic properties in soil–vegetation–atmosphere systems. In: R.A. Feddes (Editor), Space and Time Scale Variability and Interdependencies in Hydrological Processes (Int. Hydrol. Ser.). Cambridge Univ. Press, 420 pp.

Federer, C.A., 1979. A soil–plant–atmosphere model for transpiration and availability of soil water. Water Resour. Res., 15: 555–562.

Gates, D.M., 1980. Biophysical Ecology. Springer, New York, NY, 611 pp.

Giorgi, F., Marinucci, M.R. and Bates, G.T., 1993. Development of a second generation regional climate model (RegCM2). Part I: Boundary-layer and radiative transfer processes. Mon. Weather Rev., 121: 2794–2813.

Hack, J.J., Boville, B.A., Briegleb, B.P., Kiehl, J.T., Rasch, P.J. and Williamson, D.L., 1993. Description of the NCAR Community Climate Model (CCM2). NCAR Tech. Note, TN-382 + STR, 108 pp.

L'vovich, M.I., 1979. World Water Resources and their Future. AGU, Washington, DC, 415 pp.

Liang, X., Lettenmaier, D.P., Wood, E.F. and Burges, S.J., 1994. A simple hydrologically based model of land surface water and energy fluxes for general circulation models. J. Geophys. Res., 99: 14,415–14,428.

Matthews, E., 1983. Global vegetation and land use: new high-resolution data bases for climate studies. J. Clim. Appl. Meteorol., 22: 474–487.

Milly, P.C.D. and Eagleson, P.S., 1982. Parameterizations of moisture and heat fluxes across the land-surface for use in atmospheric general circulation models. MIT Rep., 279, 226 pp.

Mosley, M.P. and McKerchar, A.I., 1993. Streamflow. In: D.R. Maidment (Editor), Handbook of Hydrology. McGraw-Hill, New York, pp. 8.1–8.39.

Noilhan, J. and Planton, S., 1989. A simple parameterization of land surface processes for meteorological models. Mon. Weather Rev., 117: 536–549.

Olson, J.S., Watts, J.A. and Allison, L.J., 1983. Carbon in live vegetation of major world ecosystems. U.S. Dep. Energy, DOE/NBB-0037, No. TROO4, 152 pp.

Pilgrim, D.H. and Cordery, I., 1993. Flood runoff. In: D.R. Maidment (Editor), Handbook of Hydrology. McGraw-Hill, New York, pp. 9.1–9.42.

Pitman, A.J., Yang, Z.-L., Cogley, J.G. and Henderson-Sellers, A., 1991. Description of Bare Essentials of Surface Transfer for the Bureau of Meteorology Research Centre AGCM. BMRC Res. Rep., 32, 127 pp.

Press, W.H., Teukolsky, S.A., Vetterling, W.T. and Flannery, B.P., 1992. Numerical Recipes in Fortran. The Art of Scientific Computing. Cambridge Univ. Press, 2nd ed., 963 pp.

Rawls, W.J., Ahuja, L.R., Brakensiek, D.L. and Shirmohammadi, A., 1993. Infiltration and Soil Water Movement. In: D.R. Maidment (Editor), Handbook of Hydrology. McGraw-Hill, New York, pp 5.1–5.51.

Sellers, P.J., Randall, D.A., Collatz, G.J., Berry, J.A., Field, C.B., Dazlich, D.A. and Zhang, C., 1996. A revised land surface parameterization (SiB2) for atmospheric GCMS. Part 1: Model formulation. J. Climate, in press.

Sellers, P.J., Mintz, Y., Sud, Y.C. and Dalcher, A., 1986. A simple biosphere model (SiB) for use within general circulation models. J. Atmos. Sci., 43: 505–531.

Shao, Y. and Henderson-Sellers, A., 1996. Validation of soil moisture simulation in landsurface parameterisation schemes with HAPEX data. Global Planet. Change, 13: 11–46.

Shao, Y., Anne, R.D., Henderson-Sellers, A., Irannejad, P., Thornton, P., Liang, X., Chen, T.H., Ciret, C., Desborough, C., Balachova, O., Haxeltine, A. and Ducharne, A., 1994. Soil moisture simulation. A Report of the RICE and PILPS Workshop. IGPO Publ. Ser., 14, 179 pp.

Shuttleworth, W.J., 1993. Evaporation. In: D.R. Maidment (Editor), Handbook of Hydrology. McGraw-Hill, New York, pp. 4.1–4.53.

Wilson, M.F. and Henderson-Sellers, A., 1985. A global archive of land cover and soil data for use in general circulation climate models. J. Climatol., 5: 119–143.

Yang, Z.-L., Dickinson, R.E., Robock, A. and Vinnikov, K.Y., 1996. On validation of the snow sub-model of the Biosphere–Atmosphere Transfer Scheme with Russian snow cover and meteorological observational data. J. Climate, in press.